Postprint of: Leble S., Lewandowski W., Theoretical consideration of free convective heat transfer from a round isothermal plate slightly inclined from the vertical, INTERNATIONAL JOURNAL OF HEAT AND MASS TRANSFER, Vol. 109, (2017), pp. 835-843, DOI: 10.1016/j.ijheatmasstransfer.2017.02.034

Theoretical consideration of free convective heat transfer from a round isothermal plate slightly inclined from the vertical.

Sergey Leble* and Witold M.Lewandowski**
*Immanuel Kant Baltic Federal University,
Laboratory of Analytic -Numeric Modeling,

**Gdańsk University of Technology,
Department of Chemical Apparatus and Machinery

February 13, 2017

Abstract

A semi-analytical solution of simplified Navier-Stokes and Fourier-Kirchhoff equations describing free convective heat transfer from a round isothermal surface slightly inclined from the vertical is presented. The solution is based on the assumption, typical for natural convection, that the velocity component normal to the surface is negligibly small in comparison to the tangential one. Next we neglect the nonlinear inertia force term, but more real mass continuity is taken into account in control volume approach. This assumption do not permit to use stream function. The results for a vertical round plate in the form of the boundary layer thickness and mean Nusselt number are obtained in explicit form. They are in good agreement with literature solutions for vertical rectangular or square plates. The correction function to the Nusselt number for inclined plate is obtained in the analytical integral form that is calculated numerically and compared with the experimental values. Analysis of the results for the correction function indicate that heat transfer is greater for a positive plate inclination than for a negative one. The solution analysis also suggests that there are angles for some Rayleigh numbers at which heat transfer reaches a maximum.

Introduction

The results of theoretical and experimental studies of free convective heat transfer from heated objects of different configurations are widely published and are very useful for determining convective heat losses from apparatus, devices, pipes in industrial or energy installations, electronic equipment, buildings and so on [1]. The simplest and best-studied configuration between heated objects is the

one with a plain surface. Such surfaces represent parts of more complicated objects and are thus important in industrial applications. The geometry of flat surfaces can be different but most basic results relate to rectangular plates. There are numerous theoretical and experimental papers, the results of which are presented in [2], [3], [4] and [5]. In earlier research Lewandowski and Kubski [8], [14] presented the results of theoretical and experimental investigations for upward-facing horizontal plates and for vertical ones.

Heat transfer from a surface of circular geometry is also very important in many applications. Several experimental studies have been devoted to stationary natural convection heat transfer from such surfaces. For a horizontal plate, Kadambi and Drake [10] proposed the Nusselt - Rayleigh relation of experimental results for air. Faw and Dullforce [11] studied this same case but using interferometry. With regard to theoretical models, Schulenberg [12] proposed similarity solutions for the region around the stagnation point on a circular plate for two cases of isothermal plates and one of constant heat flux. Fujii et al. [13] presented a theoretical study of natural convection heat transfer from downward-facing horizontal surfaces with uniform heat flux. With respect to cones, Lewandowski and Leble [7], derived an analytical expression for the boundary layer thickness at the surface of a horizontal cone. This solution for an apical angle approaching π and a cone height approaching zero applies to a vertical circular plate. They also give the Nusselt-Rayleigh relation in explicit form via special functions.

Warneford and Fussey [15] performed experiments in air for a plate inclined at 85 deg from the vertical. Hassan and Mohamed studied natural convection from inclined plates and cones in [16]. In the recent experimental paper [15] Radziemska and Lewandowski presented results of experimental investigations of natural convection from circular plates facing upwards at arbitrary angles.

In the present paper we develop the theory initiated in [8] and continued in [7], by deriving approximate formulas for the natural convection boundary layer and heat transfer from discs slightly inclined at some angle α. The small parameter we introduce is simply $\tan\alpha$, and the approximations arise as expansion in power series of this parameter. Averaging along the plate surface leads to the mean Nusselt numbers (Nu) for given Rayleigh numbers (Ra) and angles in the form of ordinary integrals of local Nusselt number across the plate, parametrized by the Ra and angle, which are calculated numerically and compared with the experiments of [15], [6], [9], [18] and [19].

The first section formulates the problem. The second section establishes the model and basic equation for the boundary layer thickness. The third and fourth ones solve the basic equation with a small parameter $\tan\alpha$ and the results obtained for the zero and first approximations. The final section describes experimental studies of natural convective heat transfer from round isothermal plates in the vertical and at a slight angle to the vertical and compares them against the theory. In conclusion we point out the main practical aspects of this investigation.

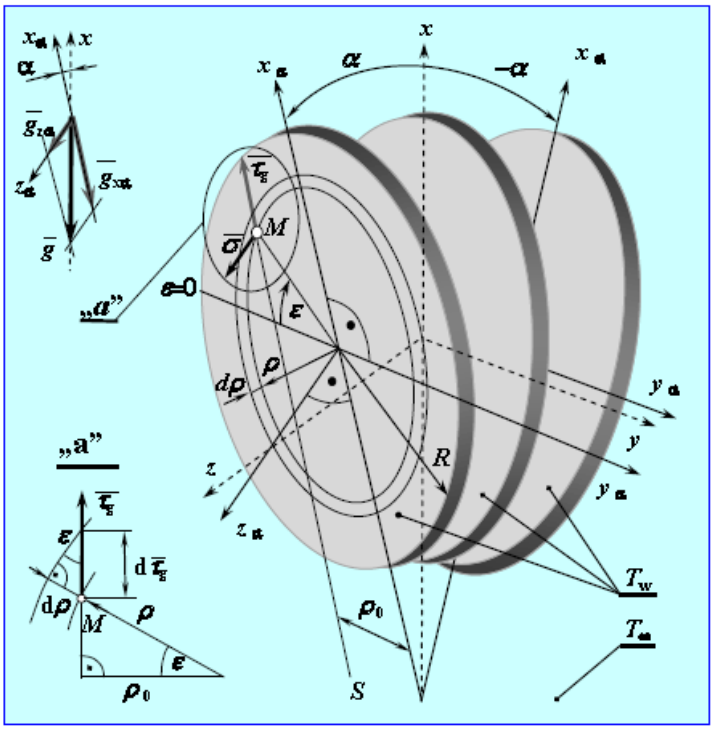

Figure 1: Coordinate system of free convective heat transfer from a sloping isothermal round plate. The black colour depicts not the thickness of the plate its thermal insulation.

1 Problem formulation

The physical model of natural convection heat transfer from a round isothermal plate at a slight angle from the vertical with proposed denotations is shown in Fig.1. The problem is 3D but the final aim of our consideration is heat transfer from the whole plate, hence the contribution of the boundary vicinity is small. Next, convection is forced by buoyancy that is x-directed, even in the case of a slightly inclined plate. Therefore we neglect derivatives with respect to y when formulating the equations. In three-dimensional local Cartesian co-ordinate space (x_α, y_α) the plate is described by the equation:

$$\frac{x_\alpha^2}{\rho^2} + \frac{y_\alpha^2}{\rho^2} = 1 \tag{1}$$

Each point on this surface is described by (x_α, y_α) that satisfy (1) or by (ρ, ϵ), where:

$$x_\alpha = \rho \cdot \sin(\epsilon) \cdot \cos(\alpha), \qquad y_\alpha = \rho \cdot \cos(\epsilon) \tag{2}$$

At any arbitrary chosen point M on the surface one can distinguish two tangent unit vectors $\overline{\tau}_\rho$ and $\overline{\tau}_\epsilon$ and one normal $\overline{\sigma}$ to the surface. The relations for the vectors $\overline{\tau_\rho}$ and $\overline{\tau}_\epsilon$ are:

$$\overline{\tau}_\rho = \frac{\partial \bar{r}}{\partial \rho}, \qquad \overline{\tau}_\epsilon = \frac{\partial \bar{r}}{\partial \epsilon} \tag{3}$$

where: $\bar{r} = (x_\alpha, y_\alpha)$

$$\overline{\tau}_{\rho x} = \frac{\partial x_\alpha}{\partial \rho} = \sin(\epsilon) \cdot \cos(\alpha), \qquad \overline{\tau}_{\rho y} = \frac{\partial y_\alpha}{\partial \rho} = \cos(\epsilon) \tag{4}$$

$$\overline{\tau}_{\epsilon x} = \frac{\partial x_\alpha}{\partial \epsilon} = \rho \cdot \cos(\epsilon) \cdot \cos(\alpha), \qquad \overline{\tau}_{\epsilon y} = \frac{\partial y_\alpha}{\partial \epsilon} = -\rho \cdot \sin(\epsilon) \tag{5}$$

The unity vector $\overline{\sigma}$ connected with $\overline{\tau}_\rho$ and $\overline{\tau}_\epsilon$, is calculated as follows:

$$\bar{\sigma} = \frac{\overline{n}}{n} \tag{6}$$

where the direction and parameter of the normal to the surface vector are:

$$\overline{n} = \bar{\tau}_\rho \times \bar{\tau}_\epsilon = \begin{bmatrix} \sin(\epsilon) \cdot \cos(\alpha) \\ \cos(\epsilon) \\ 0 \end{bmatrix} \times \begin{bmatrix} \rho \cdot \cos(\epsilon) \cdot \cos(\alpha) \\ -\rho \cdot \sin(\epsilon) \\ 0 \end{bmatrix} = \begin{bmatrix} 0 \\ 0 \\ \rho \cdot \cos(\alpha) \end{bmatrix}, \tag{7}$$

$$n = \rho \cdot \cos(\alpha) \tag{8}$$

and

$$\bar{\sigma} = \begin{bmatrix} 0 \\ 0 \\ 1 \end{bmatrix} \tag{9}$$

The choice of the variables as in the Fig.1 gives the vector of acceleration of gravity as:

$$\bar{g} = \begin{bmatrix} -g \cdot \cos(\alpha) \\ 0 \\ g \cdot \sin(\alpha) \end{bmatrix}, \tag{10}$$

which compared with (9) leads to:

$$(\bar{g}, \bar{\sigma}) = g \cdot \sin(\alpha). \tag{11}$$

The tangent unity vector $\overline{\tau}_g$ is calculated in the same way as $\overline{\sigma}$:

$$\bar{\tau}_g = \frac{\overline{s}}{s}, \tag{12}$$

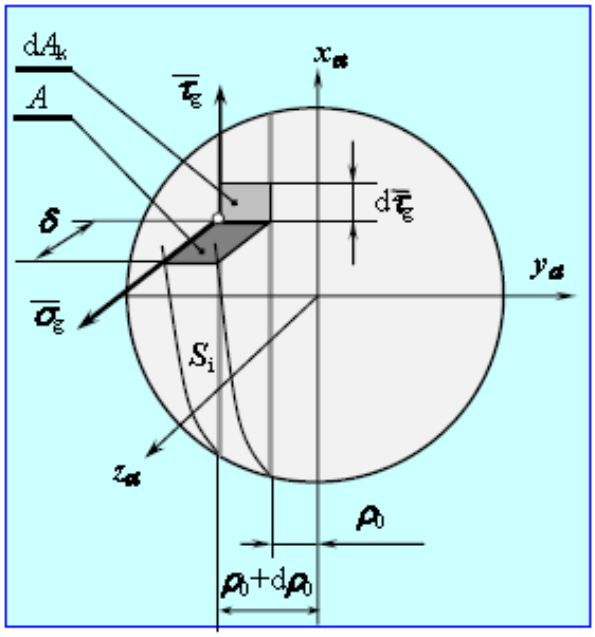

Figure 2: Graphic explanation of control surfaces A and dA_k on the heated surface under consideration.

where:

$$\overline{s} = \bar{g} - (\bar{g}, \bar{\sigma}) \cdot \bar{\sigma} = \begin{bmatrix} -g \cdot \cos(\alpha) \\ 0 \\ 0 \end{bmatrix}, \tag{13}$$

$$s = g \cdot \cos(\alpha) \tag{14}$$

and

$$\bar{\tau}_g = \begin{bmatrix} -1 \\ 0 \\ 0 \end{bmatrix} \tag{15}$$

The unit vector $\overline{\tau}_g$ determines line S on the surface (Fig.1, 2). At every point M_i the components of gravity $\overline{g}_\sigma$ and g_τ are normal and tangential to the curves S_i (Fig.2). In view of this property we decided to consider and solve the Navier-Stokes and Fourier-Kirchhoff equations, as well as the continuity, in the form of conservation laws ((33)−(37)) for the control volume limited by control surfaces A and dA_k (See Fig.2), in the two characteristic directions σ and τ.

In this notation and after applying the simplifications typical for natural convection ([1], [2], [3]):

- a fluid is incompressible and its flow is laminar, but we taken into account density variations due to temperature change (33), The last assumption do not allow to introduce stream function,
- inertia forces are negligible small in comparison with viscosity forces (see for example the equation (3.3a) from [1]),
- the physical properties of the fluid in boundary layer and in the undisturbed region (index ∞) are constant,
- the tangent to the heated surface component of the velocity inside the boundary layer is significantly greater than the normal one $W_\tau >> W_\sigma$. Two marginal regions are excluded from this assumption: 1) where the boundary layer arises $\epsilon = -\pi/2$ and 2) where it is transferred into a free buoyant plume $\epsilon = \pi/2$.
- the temperature of the lateral surface T_w is constant,
- the thicknesses of the thermal and hydraulic boundary layers are the same, and the Navier-Stokes equations can be written as:

$$\nu \cdot \frac{\partial^2 W_\tau}{\partial \sigma^2} + g_\tau \cdot \beta \cdot (T - T_\infty) - \frac{1}{\rho} \cdot \frac{\partial p}{\partial \tau_g} = 0, \tag{16}$$

$$g_\sigma \cdot \beta \cdot (T - T_\infty) - \frac{1}{\rho} \cdot \frac{\partial p}{\partial \sigma} = 0. \tag{17}$$

From equation (9) and (10) and equations (9) and (15) the normal and tangent components of gravity can be calculated as:

$$g_\sigma = \bar{\sigma} \cdot \bar{g} = \begin{bmatrix} 0 \\ 0 \\ 1 \end{bmatrix} \cdot \begin{bmatrix} -g \cdot \cos(\alpha) \\ 0 \\ g \cdot \sin(\alpha) \end{bmatrix} = g \cdot \sin(\alpha), \tag{18}$$

$$g_\tau = \bar{\tau}_g \cdot \bar{g} = \begin{bmatrix} -1 \\ 0 \\ 0 \end{bmatrix} \cdot \begin{bmatrix} -g \cdot \cos(\alpha) \\ 0 \\ g \cdot \sin(\alpha) \end{bmatrix} = g \cdot \cos(\alpha). \tag{19}$$

2 Temperature profile model

We assume that the relation for non-dimentional temperature distribution inside the boundary layer (18) is a satisfactory solution of Fourier-Kirchhoff equation [4], expressed in terms of the variable σ along the $\bar{\sigma}$:

$$\Theta = \frac{(T - T_\infty)}{(T_w - T_\infty)} = \left(1 - \frac{\sigma}{\delta}\right)^2 \quad \text{or} \quad (T - T_\infty) = \Delta T \cdot \left(1 - \frac{\sigma}{\delta}\right)^2 \tag{20}$$

The introduction (18), (19) and (20) into (16) and (17) gives:

$$\nu \cdot \frac{\partial^2 W_{\tau_g}}{\partial \sigma_g^2} + g \cdot \beta \cdot \Delta T \cdot \left(1 - \frac{\sigma}{\delta}\right)^2 \cdot \cos(\alpha) - \frac{1}{\rho} \cdot \frac{\partial p}{\partial \tau_g} = 0, \tag{21}$$

$$g \cdot \beta \cdot \Delta T \cdot \sin(\alpha) \cdot \left(1 - \frac{\sigma}{\delta}\right)^2 = \frac{1}{\rho} \cdot \frac{\partial p}{\partial \sigma}. \tag{22}$$

Integration of equation (22) for the boundary condition $\sigma = \delta$, $p_\sigma = p_{\infty(\sigma=\delta)}$ gives a formula for the pressure distribution in the boundary layer directed tangentially to the heating surface.

$$p_\sigma = p_{\infty(\sigma=\delta)} + \rho \cdot g \cdot \beta \cdot \Delta T \cdot \sin(\alpha) \cdot \left(\sigma - \frac{\sigma^2}{\delta} + \frac{\sigma^3}{3\delta^2} - \frac{\delta}{3} \right). \tag{23}$$

Pressure $p_{\infty(\sigma=\delta)}$ represents the excess of pressure over the pressure at the border of the boundary layer on the following level, which is a function of the fluid layer thickness over the heating surface. Because our considerations are concerned with unlimited space, the value of this pressure is constant.
Differentiating equation (23) with respect to τ_g (directional derivative) gives:

$$\frac{\partial p}{\partial \tau_g} = \frac{\partial p}{\partial \epsilon} \cdot \frac{\partial \epsilon}{\partial \tau_g}, \tag{24}$$

where:

$$\frac{\partial p}{\partial \epsilon} = g\beta\Delta T \sin(\alpha) \cdot \left(\frac{\sigma^2}{\delta^2} - \frac{2\sigma^3}{3\delta^3} - \frac{1}{3} \right) \frac{d\delta}{d\epsilon} \tag{25}$$

Calculation the $\partial\epsilon/\partial\tau$ is more complicated and need some explanations.
From the enlarged detail "a" in Fig.1 and Fig.2 its obvious that:

$$d\bar{\tau}_g = \frac{d\rho}{\sin(\epsilon)}, \tag{26}$$

$$\rho = \frac{\rho_0}{\cos(\epsilon)} \tag{27}$$

and

$$d\rho = \frac{\rho_0 \cdot \sin(\epsilon)}{\cos^2(\epsilon)} d\epsilon. \tag{28}$$

where: ρ_0 is the distance of the curve S from the central point of the plate (see Fig.2).

Introducing (26) into (28) leads to:

$$\frac{d\epsilon}{d\bar{\tau}_g} = \frac{\cos^2(\epsilon)}{\rho_0} \tag{29}$$

Introducing (25) and (29) into (24) gives:

$$\frac{dp}{d\tau_g} = g \cdot \beta \cdot \Delta T \cdot \sin(\alpha) \cdot \frac{\cos^2(\epsilon)}{\rho_0} \cdot \left(\frac{\sigma^2}{\delta^2} - \frac{2\sigma^3}{3\delta^3} - \frac{1}{3} \right) \frac{d\delta}{d\epsilon}. \tag{30}$$

Substituting equation (30) into equation (16) leads to:

$$\nu \cdot \frac{\partial^2 W_{\tau_g}}{\partial \sigma^2} + g\beta\Delta T \left[\cos(\alpha) \left(1 - \frac{\sigma}{\delta} \right)^2 + \sin(\alpha) \cdot \frac{\cos^2(\epsilon)}{\rho_0} \cdot \left(\frac{\sigma^2}{\delta^2} - \frac{2\sigma^3}{3\delta^3} - \frac{1}{3} \right) \frac{d\delta}{d\epsilon} \right] = 0. \tag{31}$$

For the boundary condition (for $\sigma = 0$, δ, $W_\tau = 0$) the double integration of equation (31) allows the formula of the local and next mean velocity in boundary layer to be calculated:

$$W_{\tau_g} = \frac{g \cdot \beta \cdot \Delta T \cdot \delta^2}{\nu} \cdot \left(\frac{\cos(\alpha)}{40} - \frac{\sin(\alpha) \cdot \cos^2(\epsilon)}{72 \cdot \rho_0} \cdot \frac{d\delta}{d\epsilon} \right). \tag{32}$$

The change in mass flow intensity is

$$dm = d\left(A \cdot W_{\tau_g} \cdot \rho\right), \tag{33}$$

where A is the cross-section area of the boundary layer (see Fig.2).The amount of heat necessary to cause this change in mass flux is

$$dQ = \Delta i \cdot dm = \rho \cdot c_p \cdot \left(\overline{T - T_\infty}\right) \cdot d(A \cdot W_{\tau_g}). \tag{34}$$

Substitution of the mean temperature

$$\left(\overline{T - T_\infty}\right) = \frac{1}{\delta} \cdot \int_0^\delta \Delta T \cdot \left(1 - \frac{\sigma}{\delta}\right)^2 \cdot d\sigma = \frac{\Delta T}{3} \tag{35}$$

gives

$$dQ = \frac{1}{3} \rho \cdot c_p \cdot \Delta T \cdot d(A \cdot W_{\tau_g}). \tag{36}$$

The heat flux described by equation (36) can be compared to the heat flux determined by Newton's equation (37):

$$dQ = \alpha \cdot \Delta T \cdot dA_k = -\lambda \cdot \left(\frac{\partial \Theta}{\partial \sigma_g} \right)_{\sigma_g = 0} \cdot \Delta T \cdot dA_k, \tag{37}$$

where A_k is the control surface of the heated surface (see Fig.2).

From the simplifying assumption of the temperature profile inside boundary layer (20), the dimensionless temperature gradient on the heated surface can be evaluated as

$$\left(\frac{\partial \Theta}{\partial \sigma} \right)_{\sigma = 0} = -\frac{2}{\delta}. \tag{38}$$

By substituting equation (38) into equation (37) and equating the result with equation (36), one obtains the dependence (39)

$$\frac{1}{6 \cdot \lambda} \cdot \rho \cdot c_p \cdot \delta \cdot d(A \cdot W_{\tau_g}) = dA_k. \tag{39}$$

Introduction (10) and (13) creates coordinate of the line S in three-dimensional Cartesian space.

$$s_x = -g \cdot \cos(\alpha), \;\; s_y = 0 \quad \text{and} \quad s_z = 0 \tag{40}$$

Differentiating equations (2) gives the coordinate of tangent vector to the line S:

$$\frac{dx_\alpha}{d\epsilon} = \frac{d\rho}{d\epsilon}\cdot\sin(\epsilon)\cdot\cos(\alpha)+\rho\cdot\cos(\epsilon)\cdot\cos(\alpha), \quad \frac{dy_\alpha}{d\epsilon} = \frac{dr}{d\epsilon}\cdot\cos(\epsilon)-\rho\cdot\sin(\epsilon). \tag{41}$$

Because the ratio of coordinate (40) and (41) should be constant ($s_x^{\cdot} d\epsilon/dx = s_y^{\cdot} d\epsilon/dy = s_x^{\cdot} dy/d\epsilon = s_y^{\cdot} dx/d\epsilon = 0$), one can found the equation (42) and then, after its integrating it, relationship (43):

$$\frac{d\rho}{d\epsilon} = \rho\cdot\tan(\epsilon) \tag{42}$$

From Fig.2 and relation (29) we see that the cross-sectional area (A) and the control surface (dA_k) are (see (27)):

$$A = d\rho_0\cdot\delta \tag{43}$$

$$dA_k = d\rho_0\cdot d\tau_g = \frac{d\rho_0\cdot\rho_0\cdot d\epsilon}{\cos^2(\epsilon)} \tag{44}$$

Substituting equations (32), (43) and (44) into equation (39) leads to the non-linear differential equation:

$$K^*\cdot\delta\cdot d\left(X_1\cdot\delta^3 - X_2^*\cdot\delta^3\cdot\frac{d\delta}{d\epsilon}\right) = X_3\cdot d\epsilon \tag{45}$$

where:

$$K^* = \frac{Ra_R}{6\cdot R^3} = \frac{\rho\cdot c_p}{6\cdot\lambda}.\frac{g\cdot\beta\cdot\Delta T}{\nu}, X_1 = \frac{\cos(\alpha)}{40}, X_2^* = \frac{\sin(\alpha)\cdot\cos^2(\epsilon)}{72\cdot\rho_0}, X_3 = \frac{\rho_0}{\cos^2(\epsilon)} \tag{46}$$

and the Rayleigh number is conventionally defined as:

$$Ra_R = \frac{g\cdot\beta\cdot\Delta T\cdot R^3}{\nu\cdot a}. \tag{47}$$

Equation (45) is transformed as

$$K\cdot\delta\cdot d\left(\delta^3 - X_2\cdot\delta^3\cdot\frac{d\delta}{d\epsilon}\right) = X_3\cdot d\epsilon \tag{48}$$

where the rescaled parameter K and X_2 are:

$$K = K^*\cdot X_1 = \frac{\cos(\alpha)}{40}\frac{Ra_R}{6\cdot R^3}, \qquad X_2 = \frac{X_2^*}{X_1} = .\frac{10\cdot\tan(\alpha)\cdot\cos^2(\epsilon)}{9\cdot\rho_0} \tag{49}$$

The zero approximation solution

Differentiating (48) we get the second order differential equation:

$$K \cdot \delta \cdot \left(3\delta^2 \frac{d\delta}{d\epsilon} + \left(\frac{10 \tan\alpha \cos\epsilon \sin\epsilon}{9\rho_0} \right) \delta^3 \frac{d\delta}{d\epsilon} - \left(\frac{5 \tan(\alpha) \cdot \cos^2(\epsilon)}{9 \cdot \rho_0} \right) \delta^2 \left(\frac{d\delta}{d\epsilon} \right)^2 - \left(\frac{5 \tan(\alpha) \cdot \cos^2(\epsilon)}{9 \cdot \rho_0} \right) \delta^3 \frac{d^2\delta}{d\epsilon^2} \right) \tag{50}$$

$$= \frac{\rho_0}{\cos^2(\epsilon)}.$$

Let us introduce the new variables

$$y(\epsilon) = K^{1/3} \cdot \delta \quad and \quad r = K^{1/3}\rho_0 \tag{51}$$

that gives
$3\frac{\partial y(\epsilon)}{\partial \epsilon} - \frac{r}{y^3(\epsilon)\cos^2\epsilon}$

$$- \tan\alpha \left[\frac{5\cos^2\epsilon}{9r} \left(\frac{\partial y(\epsilon)}{\partial \epsilon} \right)^2 - \frac{5\cos^2\epsilon}{9r} y(\epsilon) \frac{\partial^2 y(\epsilon)}{\partial \epsilon \partial \epsilon} + \frac{10\cos\epsilon\sin\epsilon}{9r} y(\epsilon) \frac{\partial y(\epsilon)}{\partial \epsilon} \right] = 0. \tag{52}$$

The solution for slightly inclined, round vertical plate in the first order in small parameter $\tan\alpha$ is described by the first two terms of the equation:

$$3\frac{\partial y(\epsilon)}{\partial \epsilon} - \frac{r}{(\cos^2\epsilon)(y(\epsilon))^3} = 0 \tag{53}$$

Integrating equation (53) gives:

$$y(\epsilon) = \left(\frac{4}{3} r (\tan(\epsilon) + \tan(\epsilon_m)) \right)^{1/4} \tag{54}$$

which corresponds to the original form of boundary layer thickness (compare with [5]). This fact and, general good results against experiments (see the Table.2 and plots Fig.5, Fig.6 at the end of our article) confirm the quality of approximations setup of our work.

$$\delta = \left(\frac{4}{3K} \rho_0 (\tan(\epsilon) + \tan(\epsilon_m)) \right)^{\frac{1}{4}}. \tag{55}$$

The local heat transfer coefficient is determined by:

$$\alpha_M = \frac{2 \cdot \lambda}{\delta} = 2 \cdot \lambda \cdot \left(\frac{3 \cdot K}{4 \cdot \rho_0 (\tan(\epsilon) + \tan(\epsilon_m))} \right)^{\frac{1}{4}} \tag{56}$$

The non-dimentional form of the local and subsequently of the mean value of this coefficient is expressed by the Nusselt number. The local Nusselt number $Nu_M = \frac{\alpha_M \cdot R}{\lambda}$ defines its mean value by the surface integral:

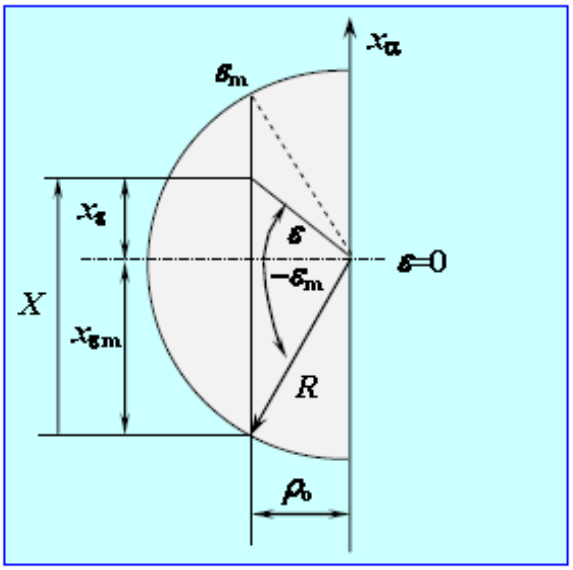

Figure 3: The definition of variables and model of their integration on the surface of the round plate.

$$\overline{Nu}_0 = \frac{1}{\pi R^2} \int_{\Sigma} Nu_M \cdot d\Sigma = \frac{2}{\pi R^2} \int_0^R d\rho_0 \int_0^{2\cdot\sqrt{R^2-\rho_0^2}} \frac{\alpha_M\left(X,\rho_0\right)\cdot R}{\lambda} dX, \qquad (57)$$

where according to Fig.3 the integration variable is defined by:

$$X = \rho_0\left(\tan(\epsilon) + \tan(\epsilon_m)\right) \qquad (58)$$

Taking into account (55) and (56) in (57) the mean Nusselt number for the whole surface of the slightly inclined vertical plate after the first differentiation gives:

$$\overline{Nu}_0 = \left(\frac{3\cdot K}{4}\right)^{\frac{1}{4}} \frac{2}{\pi\cdot R} \int_0^R \left(\int_0^{2\cdot\sqrt{R^2-\rho_0^2}} \frac{dX}{X^{\frac{1}{4}}} \right) d\rho_0 = \left(\frac{3\cdot K}{4}\right)^{\frac{1}{4}} \frac{8\cdot 2^{\frac{3}{4}}}{3\cdot\pi\cdot R} \int_0^R \left(R^2-\rho_0^2\right)^{\frac{3}{8}} d\rho_0 \qquad (59)$$

The introduction of a new variable (60) and parameters (49) into (59) leads to:

$$\left(\frac{\rho_0}{R}\right)^2 = \eta \qquad \text{and} \qquad d\rho_0 = \frac{R \cdot d\eta}{2 \cdot \eta^{\frac{1}{2}}} \tag{60}$$

$$\overline{Nu}_0 = (Ra_R \cos(\alpha))^{1/4} \frac{2}{\pi \cdot 240^{1/4}} \left(\frac{8}{3}\right)^{3/4} \int_0^1 \left(\sqrt{1-\eta}\right)^{3/4} \frac{d\eta}{\eta^{\frac{1}{2}}} \tag{61}$$

The solution of the integral in equation (61) with the use of Euler functions B and Γ takes the value:

$$\int_0^1 \left(\sqrt{1-\eta}\right)^{3/4} \frac{d\eta}{\eta^{\frac{1}{2}}} = B\left(\frac{1}{2}, \frac{11}{8}\right) = \frac{\Gamma\left(\frac{1}{2}\right)\Gamma\left(\frac{11}{8}\right)}{\Gamma\left(\frac{15}{8}\right)} = 1.652\,5 \tag{62}$$

Thus, the zero approximation solution (for $\alpha = 0$) of convective heat transfer from vertical slightly inclined round isothermal plate is:

$$\overline{Nu}_0 = \frac{2}{\pi \cdot 240^{1/4}} \left(\frac{8}{3}\right)^{3/4} \frac{2}{\pi} \cdot 1.652\,5 \cdot (Ra_R \cos(\alpha))^{1/4} = 0.557\,8 \cdot (Ra_R \cos(\alpha))^{1/4} \tag{63}$$

3 The first approximation solution

The first approximation for the boundary layer thickness is defined by:

$$y(\epsilon) = y_0(\epsilon) + (\tan\alpha)\, y_1(\epsilon), \tag{64}$$

where $y_0(\epsilon)$ is determined as the zero approximation of the theory: $y_0(\epsilon) = \left(\frac{4}{3} r (\tan(\epsilon) + \tan(\epsilon_m))\right)^{1/4}$ see equation (54). The correction term $y_1(\epsilon)\tan\alpha$ contains the small parameter $\tan\alpha$. The equation for the function $y_1(\epsilon)$ is derived by substituting (64) into (52) taking into account the first term in $\tan\alpha$

$$27r \frac{\partial y_1(\epsilon)}{\partial \epsilon} \sqrt[4]{\frac{4}{3} r (\tan\epsilon + \tan\epsilon_m)} +$$
$$-5\cos^2\epsilon \left(\frac{r^2}{3} \frac{\left(\tan^2\epsilon + 1\right)^2}{\left(\frac{4}{3} r (\tan\epsilon + \tan\epsilon_m)\right)^{\frac{7}{4}}} - \frac{2r(\tan\epsilon)}{3} \frac{\tan^2\epsilon + 1}{\left(\frac{4}{3} r (\tan\epsilon + \tan\epsilon_m)\right)^{\frac{3}{4}}} \right) \sqrt{\frac{4}{3} r (\tan\epsilon + \tan\epsilon_m)} +$$
$$-\frac{5r^2\cos^2\epsilon}{9} \frac{\left(\tan^2\epsilon + 1\right)^2}{\left(\frac{4}{3} r (\tan\epsilon + \tan\epsilon_m)\right)^{\frac{5}{4}}} + 27r^2 y_1(\epsilon) \frac{\tan^2\epsilon + 1}{\left(\frac{4}{3} r (\tan\epsilon + \tan\epsilon_m)\right)^{\frac{3}{4}}} - \frac{10r(\cos\epsilon \sin\epsilon)}{3} \frac{\tan^2\epsilon + 1}{\sqrt[4]{\frac{4}{3} r (\tan\epsilon + \tan\epsilon_m)}} =$$
$$0.$$

Transition to the variable with taking into account (52)

$$\left(\frac{4}{3} r (\tan(\epsilon) + \tan(\epsilon_m))\right)^{1/4} = \left(\frac{4}{3} K^{1/3} \rho_0 (\tan(\epsilon) + \tan(\epsilon_m))\right)^{1/4} = s \tag{65}$$

after some algebra gives the equation for $y_1(\epsilon)$:

$$81s^3\frac{\partial y_1(s)}{\partial s}+243s^2y_1(s)-20=0 \tag{66}$$

Its solution gives

$$y_1(s)=\frac{C}{s^3}+\frac{20}{81s^2} \tag{67}$$

We choose the integration constant $C=0$, cutting the leading singularity, having $y(\epsilon)=s+(\tan\alpha)\frac{20}{81s^2}$.

$$y(\epsilon)=\left(\frac{4}{3}K^{1/3}\rho_0\left(\tan(\epsilon)+\tan(\epsilon_m)\right)\right)^{1/4}+(\tan\alpha)\,y_1(\epsilon), \tag{68}$$

which corresponds to (55) and to the original form of the boundary layer thickness (compare with [5])

$$\delta=.K^{-1/3}\left(\left(\frac{4}{3}K^{1/3}\rho_0\left(\tan(\epsilon)+\tan(\epsilon_m)\right)\right)^{1/4}+(\tan\alpha)\,y_1(\epsilon)\right). \tag{69}$$

Further transformations, analogous to (56)-(59) leads to:

$$\alpha_M(X,\rho_0)=\frac{2\cdot\lambda}{K^{-1/3}\left(\left(\frac{4}{3}K^{1/3}\rho_0\left(\tan(\epsilon)+\tan(\epsilon_m)\right)\right)^{1/4}+(\tan\alpha)\,y_1(\epsilon)\right)} \tag{70}$$

$$\overline{Nu}=81\frac{12}{\pi R}\int_0^R d\rho_0\int_0^{\left(\frac{4}{3}K^{1/3}2\cdot\sqrt{R^2-\rho_0^2}\right)^{1/4}}\frac{s^5}{81s^3+20\tan\alpha}ds. \tag{71}$$

Calculating the internal integral by transition to the variable η (60) yields:

$$\overline{Nu}=\tfrac{2}{\pi}\int_0^1\left(\tfrac{4}{3}K^{1/3}2\cdot R\sqrt{1-\eta}\right)^{3/4}\frac{\cdot d\eta}{\eta^{\frac{1}{2}}}+$$
$$-\tfrac{40}{81\pi}\tan\alpha\int_0^1\left(\ln\left|\left(\tfrac{4}{3}K^{1/3}2\cdot R\sqrt{1-\eta}\right)^{3/4}+\tfrac{40}{81\pi}\tan\alpha\right|-\ln\left|\tfrac{20}{81}\tan\alpha\right|\right)\frac{d\eta}{\eta^{\frac{1}{2}}}.$$

Account for the zero approximation expression for the mean Nusselt number (61) gives:

$$\overline{Nu}=\overline{Nu}_0-\frac{40}{81\pi}\tan\alpha\int_0^1\ln\left|1+\frac{2.1472}{\tan\alpha}\left(Ra_R\cos\alpha\right)^{1/4}(1-\eta)^{\frac{3}{8}}\right|\frac{d\eta}{\eta^{\frac{1}{2}}}. \tag{72}$$

This means that the dependence the mean Nusselt number $\overline{Nu}$ on Rayleigh Ra_R takes the form:

$$\overline{Nu}=0.5578\cdot\left(Ra_R\cos(\alpha)\right)^{1/4}-\Phi(\alpha,Ra_R), \tag{73}$$

the function $\Phi(\alpha, Ra_R)$ will be presented below numerically.

In literature [20], [21], [22] and [23] the problem of natural convection from the heated inclined surfaces is considered with account of nonlinear inertia term. However the resulting system of ordinary differential equations is too complicated to be solved analytically. In the book [20] the table of velocity and temperature gradients on the plate surface is presented (Table 5.2.1, see also in the [21]). The values of the parameters are numerically calculated in the mentioned works by means of approximate expansion method at small angles of plate inclination. By means of the given table perhaps is difficult to solve practical problems.

We also obtain the nonlinear equation for the width of boundary layer 51 and solve it by the approximation method that is described above. This method allows to obtain the solution presented in our paper and may be considered as a base for engineering. The advantage of our method of the problem solution is in compact explicit form of resulting expressions. The form allows us to evaluate heat transfer intensity as function of Rayleigh number by integration over the whole palate within some inclinations range (72). This and the generally good results against experiments (see Table 2 and the plots on Figs.5 and 6 at the end of our article) confirm the quality of the approximations setup of our work.

4 The numerical evaluation against experiment

The function $\Phi(\alpha, Ra_R)$ calculated from (61) for the range of angles α from -20 to 20 deg and the Rayleigh numbers Ra_R from 10^3 do 10^8 are presented in Table 1. and Fig.4.

Table.1 The values of function $\Phi(\alpha, Ra_R)$ calculated numerically for Ra_R.= $10^3 - 10^8$ and $-20 \leq \alpha \leq 20$ deg

				$\Phi(\alpha, Ra_R)$		
α	$Ra_R = 10^3$	10^4	10^5	10^6	10^7	10^8
-20	-0.3552	-0.421 11	-0.48606	-0.550 50	-0.61464	-0.678 63
-10	-0.21283	-0.244 21	-0.27538	-0.306 43	-0.33742	-0.368 37
-5	-0.12462	-0.140 07	-0.15547	-0.170 83	-0.18619	-0.201 53
-2	-5.958E-2	-6.571 6E-2	-7.185E-2	-7. 797 2E-2	-8.409E-2	-9.021 6E-2
-1	-3.348E-2	-3.653 9E-2	-3.960E-2	-4. 266 1E-2	-4.572E-2	-4.878 1E-2
0	7.019E-5	7.325E-5	7.630E-5	7.936E-5	8.242E-5	8.548E-5
1	3.350E-2	3.655 1E-2	3.960 8E-2	4.266 5E-2	4.572E-2	4.878 2E-2
2	5.966E-2	6.576 3E-2	7.187 3E-2	7.798 7E-2	8. 410 3E-2	9.022 1E-2
5	0.12515	0.140 36	0.15563	0.170 93	0.18624	0.201 56
10	0.21498	0.245 42	0.27606	0.306 81	0.33763	0.368 49
20	0.36446	0.426 31	0.48898	0.552 14	0.61557	0.679 15

The plots below are related to the comparison of our solution with experiments. It is important to note that the experimental presentation implies recalculation of Ra and Nu on the basis of the authors' definitions. In all cited articles [6], [9], [18] and [19] on experimental studies, the authors use the diameter of the vertical plate D as a characteristic linear dimension in the Nusselt -

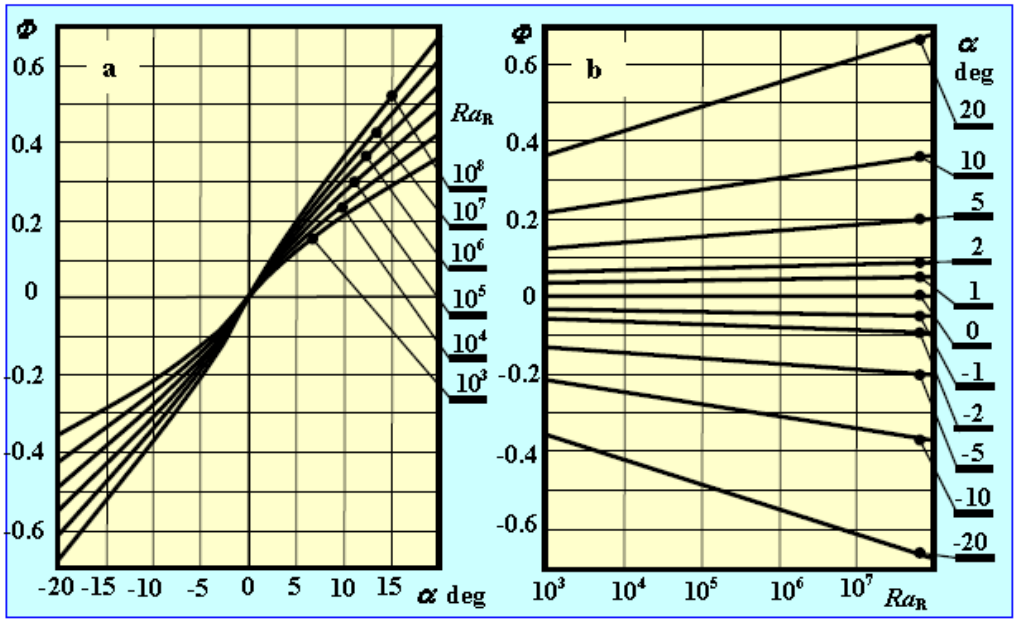

Figure 4: The plots represent results of evaluation of the correction Φ as function of angle α for given values of Rayleigh number (a) and as function of Rayleigh number for given values of the angle (b).

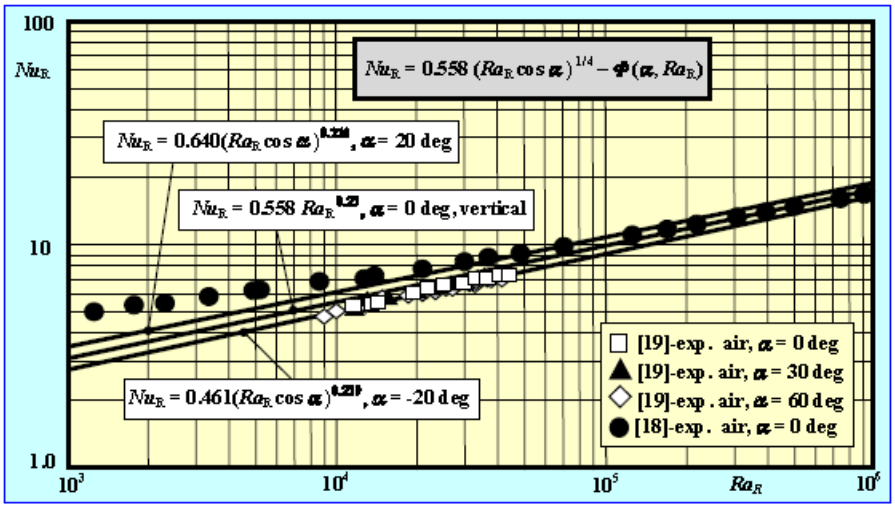

Figure 5: Theory vs. experiment [18,19] for air: the dependence of mean Nusselt number on the Rayleigh number from 10^3 till 10^6 for zero and ± 20 deg angles

Rayleigh relation (compare with our definition 61). Therefore, we have recalculated all experimental points of Ra_D and criterion relations $Nu_D = C_D Ra_D^{1/4}$ in Figs 5, 6 using the factors $Ra_R = Ra_D/2^{1/4}$ and $Nu_R = (C_D/2^{1/4})Ra_R^{1/4}$.

Recalculated in this way the analytical, numerical and experimental results of other authors lead to Nusselt -Rayleigh relations which are converge with our solution for limiting case of inclined plate - vertical ones ($\overline{Nu} = 0.558\,Ra_R^{1/4}$):

$\overline{Nu} = 0.461\,Ra_R^{1/4}$ analytical solution [6] (-17.4%),

$\overline{Nu} = 0.484\,Ra_R^{1/4}$ experiments for water (-15.3%), $\overline{Nu} = 0.551 Ra_R^{1/4}$ (-1.3%) experiments for air $D = 0.07m$ [6] ,

$\overline{Nu} = 0.587\,Ra_R^{1/4}$ numerical solution [6] (+4.9%),

$\overline{Nu} = 0.642\,Ra_R^{1/4}$ analytical solution of horizontal cone for apex angle zero (vertical plate) [7] (+13.1%),

$\overline{Nu} = 0.336\,Ra_R^{1/4}$ the mean correlation of all results of free convection in water [9] (-66.1%). The discrepancy is the last case is explained by the method that the authors used to average all measurement results obtained for inclined round plates with a slope varying from $\alpha = 0$ (vertical) to $\alpha = \pi/2$ (horizontal position).

In papers [18] and [19] the exponents n in Nusselt-Rayleigh relations are different from $n \neq 1/4$ which does not allow one to convert them using the factor $2^{1/4}$.Accordingly, individual experimental dots of Ra values in Fig 5 and Fig. 6 were respectively converted according to the formula:$Ra_{Ri} = Ra_{Di}/2^{1/4}$.

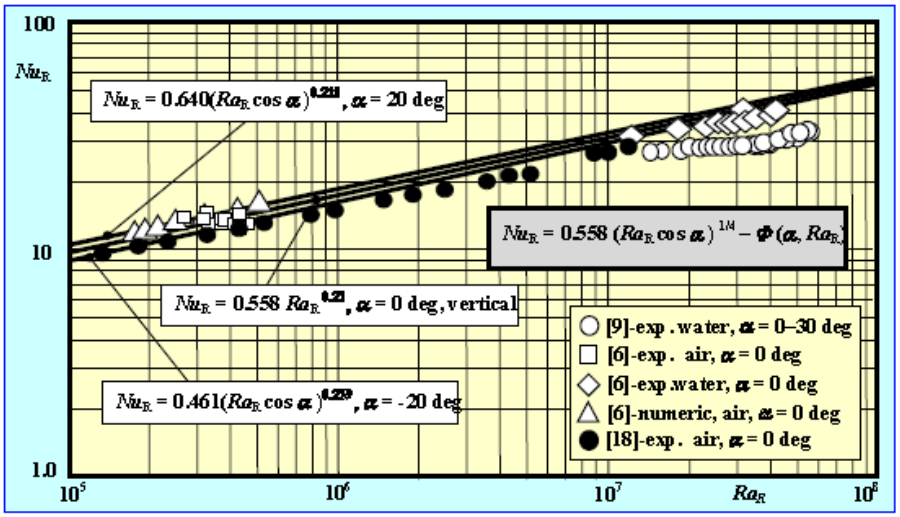

Figure 6: Theory vs. experiment and numerics [6, 9, 18]: the dependence of the mean Nusselt number on the Rayleigh number from 10^5 till 10^8 for zero and ± 20 deg angles.

Both figures present the results of measurements of free convective heat transfer from isothermal round plates in vertical or inclined position mainly in air and water [6], [9]. For better presentation, the wide of Rayleigh numbers range is divided in two parts from 10^3 till 10^6 and from 10^5 till 10^8 - to include the results of Hassani and Hollands [18].

To validate the theoretical results on the basis of (72), (73) we numerically build the correspondent Tables 1 and 2. and plot dependences in the conventional form of mean Nusselt - Rayleigh numbers relations. For better presentation we show the solution for a vertical plate $\alpha = 0$

$\overline{Nu}_R = 0.558 Ra_R^{0.25}$

and for border values of angles $\alpha = \pm 20\,\mathrm{deg}$

$\overline{Nu}_R = 0.461 Ra_R^{0.259}$ for $\alpha = -20\,\mathrm{deg}$ and $\overline{Nu} = 0.640 Ra_R^{0.218}$ for $\alpha = 20\,\mathrm{deg}$.

Table.2 The values of mean Nusselt numbers $\overline{Nu}$ calculated numerically from (72), (73) for $10^3 \le Ra_R \le 10^8$ and $-20 \le \alpha \le 20$ deg

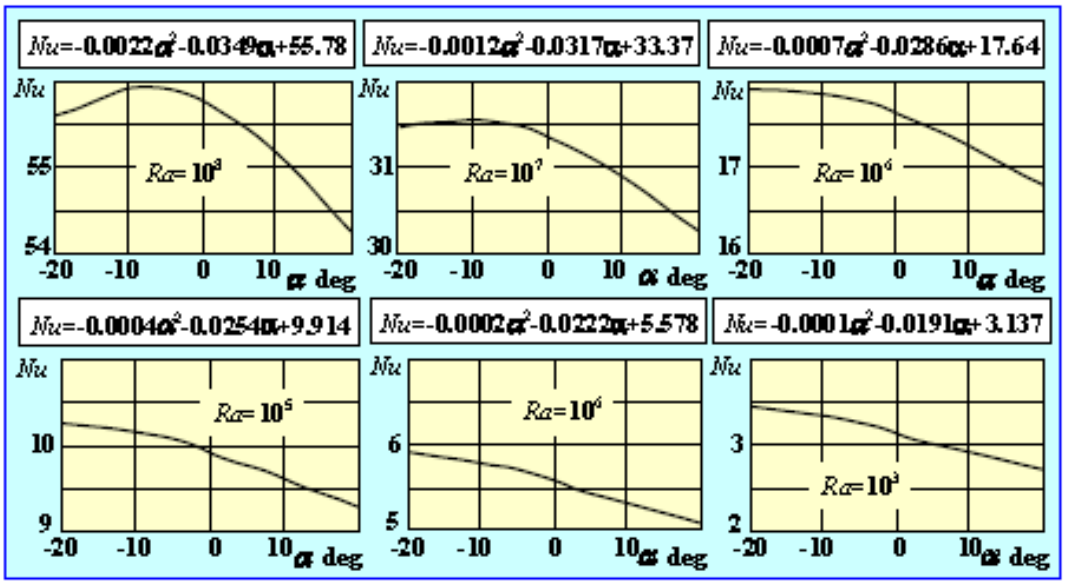

Figure 7: Plots showing the dependences of the mean Nusselt number on angles for a given Rayleigh number in graphical and algebraic form.

			$\overline{Nu}$			
α	$Ra_R = 10^3$	10^4	10^5	10^6	10^7	10^8
-20	3, 4435	5, 913	10, 252	17, 918	31, 498	55, 598
-10	3, 3376	5, 8009	10, 157	17, 878	31, 585	55, 935
-5	3, 2584	5, 7128	10, 065	17, 793	31, 524	55, 928
-2	3, 1958	5, 6429	9, 9896	17, 714	31, 447	55, 862
-1	3, 1701	5, 6143	9, 9585	17, 681	31, 412	55, 827
0	3, 1367	5, 5779	9, 9192	17, 639	31, 367	55, 780
1	3, 1031	5, 5412	9, 8793	17, 596	31, 32	55, 729
2	3, 0766	5, 5114	9, 8459	17, 559	31, 279	55, 681
5	3, 0086	5, 4323	9, 7542	17, 451	31, 151	55, 525
10	2, 9098	5, 3113	9, 6053	17, 265	30, 910	55, 198
20	2, 7239	5, 0656	9, 2772	16, 815	30, 268	54, 24

The results definitely point a more effective heat exchange for inclined plates of positive angles compared with vertical one. The opposite situation gives less effective convective heat transfer, as clearly evident from our theoretical solution (72) because the extra term Φ is proportional to the odd function of α.

This conclusion encouraged us to investigate the dependence of the correction term on α and Ra_R in more details. The results of these investigations are shown in Fig.7.

The resulting plots at some Rayleigh numbers exhibit maximum of the func-

tion $\overline{Nu}(\alpha)$, which allows the optimal angle of inclination of the heated plate to be chose for practical use. This conclusion, however, requires experimental confirmation.

5 Conclusion

To conclude, we wish to stress that the main result of our investigation, the rather compact formulas (72) and (73), is validated by theoretical and experimental analysis in the validity range -20 deg $< \alpha < 20$ deg. The results of numerical evaluation and graphical presentation give the user tool for practical application in engineering for a given angle and Rayleigh number ranges.

Analysis of our solution also indicate that heat transfer is greater for a positive plate inclination ($\alpha < 0$) than for a negative one ($\alpha > 0$) and that are angles for some Rayleigh numbers at which heat transfer reaches a maximum.

Equation (52), which we derived in this paper, gives a more exact dependence of the correction on angle α and Rayleigh number, but its order is two and the presence of non-linearity seriously complicates its solution. Moreover, the validity of the whole theory is restricted by the approximation we used: for large angles it is necessary to take both velocity components into account.

6 Nomenclature

a	thermal diffusivity (m^2/s)
A	control surface across the boundary layer (m^2)
B	Euler function (62) (-)
c_p	specific heat at constant pressure (J/(kg·K))
dA_k	control surface of heated surface (m^2)
g	acceleration due to gravity (m/s^2)
K	parameter (49) (-)
m	..mass (kg)
$Nu = \frac{\alpha \cdot R}{\lambda}$	Nusselt number (-)
Q	heat flux (W)
p	pressure (N/m^2)
R	radius of the plate (m)
Ra	Rayleigh number (47) (-)
T	temperature (^{o}C or K)
ΔT	temperature difference (K)
W	velocity of the fluid (m/s)
x, y, z	Cartesian co-ordinates and distances (m)
X	integration variable (58) and Fig.3
Greek symbols	
α	angle of plate inclination (deg)
α	heat transfer coefficient ($W/(m^2 \cdot K)$)
β	average volumetric thermal expansion coefficient (1/K)

δ	boundary layer thickness (m)
ϵ	angular coordinate (deg)
λ	thermal conductivity of the fluid (W/mK)
ν	kinematic viscosity of the fluid (m^2/s)σ
ρ	radial distance (m)
σ	normal to the surface unity vector (-)vector
τ	tangent to the surface unity vector (-)
Γ	Euler function (62) (-)
Θ	dimensionless temperature defined by (20) (-)

References

[1] Y.Jaluria.:Natural Convection Heat and Mass Transfer; Pergamon Press, Oxford, 1980.

[2] Latif M. Jiji.: Heat Convection, Springer-Verlag Berlin Heidelberg, 2009.

[3] M.Favre-Marinet, S.Tardu, Convective Heat Transfer. Solved Problems, ISTE Ltd, John Wiley & Sons, Inc., 2009

[4] Bosworth, R. L. C., Heat Transfer Phenomena, Wiley, New York, 1952.

[5] S.W.Churchill.: Free convection around immersed bodies, 2.5 Single - Phase Convective Heat Transfer Hemisphere Publishing Corporation, 1983.

[6] W.M.Lewandowski, E.Radziemska; Heat transfer by free convection from an isothermal vertical round plate in unlimited space, Applied Energy 68 (2001) 347-366

[7] S.Leble, W.M.Lewandowski, A theoretical consideration of a free convective boundary layer on an isothermal horizontal conic, Applied Mathematical Modelling 28 (2004) 305-321

[8] W.M. Lewandowski.: Natural convection heat transfer from plate of finite dimensions, International Journal of Heat and Mass Transfer, Vol. 34, No. 3, 1991, pp. 875–885

[9] E.Radziemska, W.M.Lewandowski; Experimental Investigations of Natural Convection from Circular Plates at Variable inclination, JOURNAL OF THERMOPHYSICS AND HEAT TRANSFER Vol. 21, No. 4, October–December 2007

[10] Kadambi, V., and Drake, R. M., "Free Convection Heat Transfer from Horizontal Surfaces for Prescribed Variations in Surface Temperature and Mass Flow Through the Surface," Princeton University, TR Mechanical Engineering HT-1, 1960.

[11] Faw, R. E., and Dullforce, T. A., "Holographic Interferometric Measurement of Convective Heat Transport Beneath a Heated Horizontal Circular Plate in Air," International Journal of Heat and Mass Transfer, Vol. 25, No. 8, 1982, pp. 1157–1166.

[12] Schulenberg, T., "Natural Convection Heat Transfer Below Downward-Facing Horizontal Surfaces," International Journal of Heat and Mass Transfer, Vol. 28, No. 2, 1985, pp. 467–477

[13] Fujii, T., Honda, H., and Morioka, I., "A Theoretical Study of Natural Convection Heat Transfer from Downward-Facing Horizontal Surfaces with Uniform Heat Flux," International Journal of Heat and Mass Transfer, Vol. 16, No. 3, 1973, pp. 611–62

[14] Lewandowski, W. M., and Kubski, P., "Methodical Investigation of Free Convection from Vertical and Horizontal Plates," Wärme-und Stoffübertagung, Vol. 17, No. 3, 1983, pp. 147–154.

[15] Warneford, I. P., and Fussey, D. E., "Natural Convection from a Constant-Heat-Flux Inclined Flat Plate," Proceedings of the Fifth International Heat Transfer Conference, 1974.

[16] Hassan, K. E., and Mohamed, S. A., "Natural Convection at Inclined Plates and Cones," PCH. Physico-Chemical Hydrodynamics, Vol. 5, Nos. 2/4, 1984, pp. 299.

[17] Al-Arabi, M., and El-Riedy, M., "Natural Convection Heat Transfer from Isothermal Horizontal Plates of Different Shapes," International Journal of Heat and Mass Transfer, Vol. 19, No. 12, 1976, pp. 1399–1404.

[18] A.V.Hassani, K.G.T.Hollands, A simple method for estimating natural convection heat transfer from bodies of arbitrary shape, 24th National Heat Transfer Conference, Pittsburg, Pennsylvania, August 9-12, 1987.

[19] C.J.Kobus, G.L.Wedekind, An empirical correlation for natural convection heat transfer from thin isothermal circular disks at arbitrary angles of inclination, International Journal of Heat and Mass Transfer 45 (2002) 1159-1163.

[20] B.Gebhart, Y.Jaluria, R.I.Mahajan, B.Sammakia, Buoyancy-Inducted Flows and Transport, Springer, (1988).

[21] Hasan, M. M., and Eichhorn, R. (1979). J. Heat Transfer 101, 642.

[22] Sparrow, E. M ., and Yu, H. S. (1971). J. Heat Transfer 93, 328.

[23] Minkowycz, W. J., and Cheng, P. (1976). Int. J. Heat Mass Transfer 19, 805.